

## Research Article:

Immunoregulatory Properties of Arteether in Folic Acid-Chitosan-Fe<sub>3</sub>O<sub>4</sub> Composite Nanoparticle in 4T1 Cell Line and Mice Bearing Breast CancerHajar Rajaei<sup>1</sup>, Mirza Ali Mofazzal Jahromi<sup>2</sup>, Nima Khoramabadi<sup>3</sup>, Zuhair Mohammad Hassan<sup>1\*</sup>

1. Department of Immunology, Faculty of Medical Sciences, Tarbiat Modares University, Tehran, Iran.

2. Department of Advanced Medical Sciences and Technologies, School of Medicine, Jahrom University of Medical Sciences, Shiraz, Iran.

3. Department of Bacteriology, Faculty of Medical Sciences, Tarbiat Modares University, Tehran, Iran.



**Citation** Rajaei H, Jahromi MAM, Khoramabadi N, Hassan ZM. Immunoregulatory Properties of Arteether in Folic Acid-Chitosan-Fe<sub>3</sub>O<sub>4</sub> Composite Nanoparticle in 4T1 Cell Line and Mice Bearing Breast Cancer. *Immunoregulation*. 2020; 2(2):89-102. <http://dx.doi.org/10.32598/Immunoregulation.1.4.207>

**doi** <http://dx.doi.org/10.32598/Immunoregulation.1.4.207>

**Article info:**

Received: 20 Jun 2018

Accepted: 27 Oct 2018

Available Online: 01 Jan 2020

**Keywords:**

Arteether, Nanosystem, Chitosan, Folic acid, Breast cancer

**ABSTRACT**

**Background:** Many studies have focused on the potent anti-cancer activity of Arteether (ARE). However, the hydrophobic property of this drug limits its application. To increase the bioavailability of ARE, we formulated a Nanosystem (NS) of Folic Acid (FA), Chitosan (CS), and Fe<sub>3</sub>O<sub>4</sub> for delivery of ARE into breast cancer.

**Materials and Methods:** The CS-coated Fe<sub>3</sub>O<sub>4</sub> was synthesized by co-precipitation of Fe<sup>2+</sup> and Fe<sup>3+</sup> in CS gel-like solution. Then, it was conjugated with FA and ARE. The properties of ARE loaded Nanoparticles (NPs) were characterized by Dynamic Light Scattering (DLS), Fourier Transform-Infrared (FTIR) spectra, Scanning Electron Microscopy (SEM), drug loading efficiency, and drug release. The bioactivity of this complex was evaluated in vitro and in vivo settings. Tumor volume was measured, and the cytokines of Interferon-gamma IFN-γ and interleukin 4 (IL-4) were assessed in mice splenocytes.

**Results:** DLS showed an average size of 198nm and the charge of about -7mV. FTIR confirmed the formation of ARE loaded NPs and SEM indicated its solid, dense structure. The drug exhibited a loading capacity of (20%) and significant release in citrate buffer with pH 5.4 compared with phosphate-buffered saline with pH 7.4. The NS showed significant inhibitory effect on the growth of 4T1 cell line and tumor volume. It also augmented IFN-γ and IL-4 production in breast cancer-bearing mice. ARE in FA-CS-Fe<sub>3</sub>O<sub>4</sub> composite NPs may significantly suppress tumor growth.

**Conclusion:** This NS can be utilized in the nano-based drug delivery system for the treatment of breast cancer.

**\* Corresponding Author:**

Zuhair Muhammad Hassan, PhD.

Address: Department of Immunology, Faculty of Medical Sciences, Tarbiat Modares University, Tehran, Iran.

Phone: +98 (912) 3908086

E-mail: hasan\_zm@modares.ac.ir

## Introduction

**A**rteether (ARE) is a hydrophobic ether derivative of Artemisinin (ARM). It has been known as a remarkable candidate for anti-malarial and anti-neoplastic drugs [1-3]. Tu and associates discovered ARM in the 1970s.

It was extracted from a Chinese herbal medicine called *Artemisia Annua* [4, 5]. ARM and its derivatives such as ARE signify anti-proliferative impacts on tumor cells and induce apoptosis [6-11]. They also cause cellular damage in tumor cells by generating reactive oxygen species [12]. They are sesquiterpene lactones containing an endoperoxide linkage, which reacts with ferrous iron to form free radicals [13-15]. Since the production of free radicals causes molecular damage and ultimately cell death, the use of this drug has shown promising results in cancer. By binding holotransferrin to the transferrin receptor, intake of iron will occur. Higher expression of transferrin receptors is observed on the tumor cells as compared with normal cells; therefore, higher concentrations of intracellular ferrous iron will be present in cancer cells [16-18].

As a result, cancer cells will be more susceptible to free radical formation of ARE. Despite the potent anti-cancer properties, ARE is insoluble in aqueous solutions [2]. Hence, reduced bioavailability and stability in vivo are the major obstacles for its clinical use. We decided to assess whether the encapsulation of this potent anti-cancer drug could stimulate the immune response against breast cancer along with an increase in its bioavailability. An efficient immune response against tumor would shift T lymphocyte cells to type-I and subsequently generate gamma-interferon (IFN- $\gamma$ ). The production of IFN- $\gamma$  by T Helper 1 (Th1) activates the cytotoxic T cells, and they would consequently be converted into the effector cells. These processes ultimately strengthen the immune response against tumor cells [19, 20]. As a result, encapsulation of this drug in biodegradable and biocompatible composites such as nanocarriers could be helpful in drug delivery across cancer cells [21].

In the current investigation, a nanocarrier composed of three components of  $\text{Fe}_3\text{O}_4$ , Chitosan (CS) and Folic Acid (FA) was synthesized. Nanotechnology has revolutionized the concepts of drug delivery [22]. In recent decades,  $\text{Fe}_3\text{O}_4$  application in biomedical sciences such as Magnetic Resonance Imaging (MRI), hyperthermia, and drug delivery has gained increasing interest [23-25]. Since bare  $\text{Fe}_3\text{O}_4$  has a large surface-area-to-volume ratio, it could be a right candidate as a cross-linker between CS polymers for drug entrapping. Also, it may increase the anti-cancer effect of drugs and reduce the resistance

of tumor cells to drugs [26]. CS has attracted a great deal of attention owing to its properties such as biodegradability and biocompatibility [27, 28]. It is a deacetylated biopolymer of chitin obtained from crustaceans shells [29]. The gel-like property and pH-dependent degradation of CS make it well suited as a delivery vehicle to release the loaded drug in the acidic tumor microenvironment [30].

The present study is focused on directed delivery of ARE to breast cancer cells to decrease the probable side effects of the drug, concentrate it around the tumor, and increase its therapeutic effects. To improve the delivery of the anti-tumor agent, we coupled CS- $\text{Fe}_3\text{O}_4$  composite with FA whose receptors are widely expressed on the surface of cancer cells. Consequently, uptake of FA conjugates occurs through receptor-mediated endocytosis [31, 32]. In the current investigation, we tried to load ARE in the mentioned nanoformulation to release it in the tumor microenvironment or inside the tumor cells to generate a potent immune response.

## Materials and Methods

About 6 to 8 week old female BALB/c mice were procured from the animal production center of Pasteur Institute of Iran (Karaj, Iran). The 4T1 cell line was obtained from the National Cell Bank of Iran.

### Preparation of CS- $\text{Fe}_3\text{O}_4$

CS- $\text{Fe}_3\text{O}_4$  was synthesized by co-precipitation method. About 1.5g of CS with molecular weight of 100-300kDa (Sigma-Aldrich, USA) was dissolved in 100mL 0.05M acetic acid (Merck, Germany), and then 3.51g of  $\text{FeCl}_3 \cdot 6\text{H}_2\text{O}$  and 1.29g of  $\text{FeCl}_2 \cdot 4\text{H}_2\text{O}$  (Sigma-Aldrich, USA) were added to the solution of CS and stirred for 6h at 80°C under  $\text{N}_2$  atmosphere. Subsequently, 6mL of (25%)  $\text{NH}_4\text{OH}$  (Merck, Germany) was added to the solution and stirred for 30 min. After collecting the precipitate with a strong magnet and washing with DW and (96%) ethanol (Merck, Germany), CS- $\text{Fe}_3\text{O}_4$  was dried in an oven at 35°C.

### Preparation of ARE-loaded FA-CS- $\text{Fe}_3\text{O}_4$

About 20mg/mL of CS- $\text{Fe}_3\text{O}_4$  was dispersed in DW with the final volume of 50mL at 300rpm for 30min using homogenizer (Heidolph, Germany). Then, 2.5mg/mL FA (Sigma-Aldrich, USA) in 20mL DW and 200 $\mu\text{L}$  NaOH (1 N) was added to the CS- $\text{Fe}_3\text{O}_4$  solution and stirred for 24h. Afterward, 7mg/mL ARE (Exim-Pharm International, India) in the solvent of (70%) ethanol (Merck, Germany) with the volume of 50mL was

added to the solution and stirred for 24h. The obtained solution was washed with DW, collected by a strong magnet and dried in the oven. The ARE-loaded FA-CS-Fe<sub>3</sub>O<sub>4</sub> powder was dissolved in DW under vigorous sonication for 15min using WUC D10H sonicator (Dihan, South Korea). Ultimately, the whole nanosystem (NS) contained FA-CS-Fe<sub>3</sub>O<sub>4</sub> composite NP, and the entrapped ARE (Figure 1). Preparation of FA-CS-Fe<sub>3</sub>O<sub>4</sub> NPs (without ARE) was carried out using the same method mentioned above.

### Physical characteristics of NPs

Fourier Transform-Infrared (FTIR) spectra of loaded NPs, ARE, FA, CS, and Fe<sub>3</sub>O<sub>4</sub> were obtained using an IR spectrophotometer (Nicolet IR100, Thermo, USA). Size and potential charge of ARE-loaded FA-CS-Fe<sub>3</sub>O<sub>4</sub> NPs were evaluated by Dynamic Light Scattering (DLS) using a Zetasizer and scattering particle size analyzer (Malvern, UK). Scanning electron microscopy (SEM) (JSM-6700F, JEOL, Japan) was used to characterize and confirm the size and shape of ARE-loaded FA-CS-Fe<sub>3</sub>O<sub>4</sub> NPs. The samples were combined with pure potassium bromide (KBr) for the background, and by a manual tablet press, it was compressed into discs.

### Determination of loading efficiency

About 1 mg/mL of FA-CS-Fe<sub>3</sub>O<sub>4</sub> NPs was dispersed in Phosphate-Buffered Saline (PBS) solution. Afterward, 5 mg/mL of ARE in the solvent of (70%) ethanol (Merck, Germany) was added to it and stirred at RT for 24 h (IKA, Sweden). The ARE-loaded FA-CS-Fe<sub>3</sub>O<sub>4</sub> composite was centrifuged at 5800g for 15 min (Hermle, Germany). The solution was then analyzed using ultraviolet-visible (UV) spectroscopy (Shimadzu, Japan) to determine the nonencapsulated ARE at 250nm and then compared with the standard curve prepared by using different concentrations of ARE (0.00975), (0.0195), (0.039), (0.0758), (0.15), (0.313), (0.625), (1.25), (2.5), and (5mg/mL). The amount of nonencapsulated drug was compared to the total drug in the solution of FA-CS-Fe<sub>3</sub>O<sub>4</sub> NPs and quantified as follows [28]:

$$Z=[(A-B)/A] \times 100$$

$$Y=[(A-B)/C] \times 100$$

Where Z is the drug loading efficiency percentage, Y refers to the drug loading capacity percentage, A denotes the total amount of added drug, B is the amount of free drug in solution, and C refers to the total amount of NS containing ARE and FA-CS-Fe<sub>3</sub>O<sub>4</sub> NPs.

### In vitro drug release

The drug release response of ARE-loaded FA-CS-Fe<sub>3</sub>O<sub>4</sub> NPs was studied in physiologic pH 7.4 and acidic pH 5.4, which represents the endolysosomes pH of cancer cells. Two sets of 7mg of ARE-loaded FA-CS-Fe<sub>3</sub>O<sub>4</sub> were distributed in 7mL of 0.01M PBS solution (pH 7.4) and 7mL of 0.1M citrate buffer (pH 5.4), separately. The whole volume of each buffer with the content of ARE-loaded FA-CS-Fe<sub>3</sub>O<sub>4</sub> was dispensed into 14 microtubes, containing a volume of 500 µL in duplicate in 7 various sets. Then, all sets were incubated at 37°C under gentle rotation. At exact time intervals of (2, 4, 6, 12, 24, and 48h), the samples were centrifuged at 5800g for 15min. Then, the analysis of the solution and the quantification were carried out with UV spectroscopy (Shimadzu, Japan) at a wavelength of 250nm as pointed out here [33]:

$$D_r=(R/T) \times 100$$

Where D<sub>r</sub> is the percentage of drug release, R is the amount of released ARE, and T denotes the amount of total ARE in NS.

### Cell culture

The 4T1 cells were cultured in Dulbecco's Modified Eagle Medium (DMEM) (Gibco, USA) with additive of 2mM L-glutamine and (10%) fetal bovine serum (FBS) (Gibco, USA), 100U/mL penicillin and 100µg/mL streptomycin solution (Gibco, USA) in (5%) CO<sub>2</sub> at 37°C (Gallenkamp, UK).

### Cytotoxicity assay

The cytotoxic activity of ARE and ARE-loaded NPs were evaluated by MTT "3-(4, 5-dimethylthiazol-2-yl)-2, 5-diphenyl tetrazolium bromide" (Merck, Germany) assay. About 1×10<sup>4</sup> 4T1 cells in each well with a volume of 200µL DMEM, containing (10%) FBS, 100U/mL penicillin, and 100µg/mL streptomycin solution (Gibco, USA), were seeded on two separate 96-well cell culture plates (Grinner, Germany). After 24h, they were treated with serial dilutions of 30, 45, 60, 75, 90, 105, 120, 135, and 150µg/mL of ARE, 120, 180, 240, 300, 360, 420, 480, 540 and 600µg/mL of FA-CS-Fe<sub>3</sub>O<sub>4</sub>, and 150, 225, 300, 375, 450, 525, 600, 675, 750µg/mL of ARE-loaded FA-CS-Fe<sub>3</sub>O<sub>4</sub> "each concentration contained (20%) are according to loading capacity". Then, MTT at a final concentration of 0.5mg/mL was added to each well after passing 24h and 48h the treatments being exposed to cells. Then after 4h incubation and discarding the medium of each well, 100 µL dimethyl

sulfoxide (Merck, Germany) was used to dissolve the blue formazan crystals. The absorbance was assessed at 540nm using Enzyme-Linked Immunosorbent Assay (ELISA) reader (Multiskan, Finland). The cell viability was reported as the percentage of control, as shown here:

$$V=(S/C)\times 100$$

Where V is the viability percentage, S is the Optical Density (OD) of samples (the cell lines which were treated with drug), and C is OD of the controls (the untreated cell lines).

### Tumor induction and its volume measurement

Six to eight week old female BALB/c mice were injected subcutaneously with  $6\times 10^5$  4T1 cells in 100 $\mu$ L PBS (Figure 2). After 12 days during which tumors reached a measurable size, the tumor size was measured, and the treatment was initiated. A total of 25 BALB/c mice were randomly divided into five groups, with 5 mice in each group. Groups were treated with cyclophosphamide (Sigma-Aldrich, USA) as a positive control, ARE, FA-CS-Fe<sub>3</sub>O<sub>4</sub>, ARE-loaded FA-CS-Fe<sub>3</sub>O<sub>4</sub> in PBS and the final group as a negative control (not treated at all). The mice were injected via intraperitoneal route with 0.1 mL of ARE (20mg/kg) in PBS (Merck, Germany), 0.1 mL FA-CS-Fe<sub>3</sub>O<sub>4</sub> (20mg/kg) in PBS, 0.1mL ARE-loaded FA-CS-Fe<sub>3</sub>O<sub>4</sub> (20mg/kg) in PBS, and 20mg/kg cyclophosphamide, every other day on days 12, 14, and 16. The tumor size of mice was reported on days 12, 14, 16, and 18. The tumor volume of each group was checked using a digital caliper vernier (Mitutoyo, Japan) and calculated with the following formula [34]:

$$V_t=(\pi/6)\times LW^2$$

Where  $V_t$  is the tumor volume,  $\pi$  is 3.14, L is the length of tumor tissue, and W is the tumor width.

On day 21, the mice were killed by cervical dislocation method, and various immunoassays were carried out.

### Preparation of tumor lysis antigen

The tumor tissue sample was obtained from BALB/c mouse burdening tumor in the volume of 3000 mm<sup>3</sup>. The tumor tissue was sliced into small pieces in 10 mL PBS. The specimen was lysed using the freeze-thaw procedure 5 times. Then, for deactivating serine proteases, 1 mM Phenylmethylsulfonyl Fluoride (PMSF) (Gibco, USA) was added and then sonicated with a rating power of 4 W. The cell lysate was centrifuged at 3000g for 15 min at 4°C, and the supernatant was dialyzed via dialysis bag with MW cutoff point of 3500 gmol<sup>-1</sup> (Spectra/Por, USA) for 24h. The extract was passed through a 0.22 $\mu$ m filter (GVS, USA). Bradford method was used to determine the protein concentration using the Bio-Rad assay kit, and the extract was maintained at -20°C for further use.

### Cytokine assay

On day 21, the mice were killed by cervical dislocation method, and their spleens were aseptically homogenized. Splenocytes were collected and cultured with the amount of  $1\times 10^6$ /mL in each well in Roswell Park Memorial Institute (RPMI)-1640 medium culture. The culture was complemented with 2mM L-glutamine, (10%) FBS (Gibco, USA), 100U/mL penicillin, and 100 $\mu$ g/mL streptomycin solution (Gibco, USA) in 24-well culture plates (Nunc, Denmark) with the exposure of 20 $\mu$ g/mL tumor lysis antigen. After passing three days of incubation, the supernatants of cultured spleen cells were kept at 37°C in humidified (5%) CO<sub>2</sub> (Gallenkamp, UK). The concentration of IFN- $\gamma$  and IL-4 cytokines were checked using ELISA technique. An ELISA kit (R&D, USA) was purchased to measure IFN- $\gamma$  and IL-4, and all the steps were done according to the manufacturer's protocol.

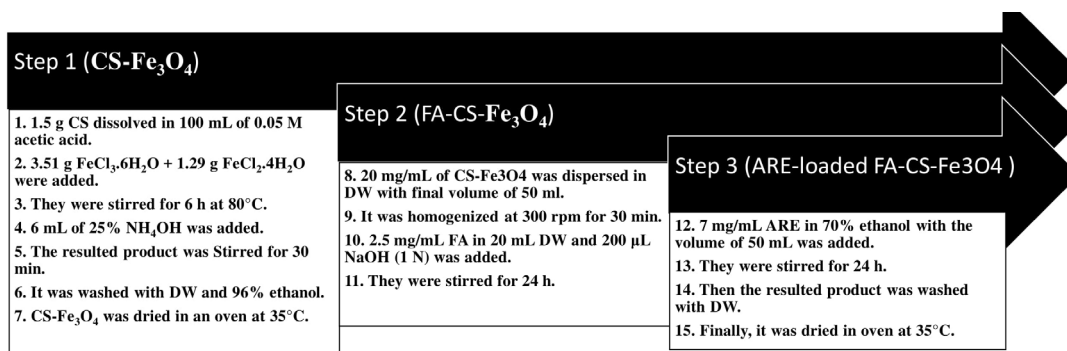


Figure 1. The process of ARE-loaded FA-CS-Fe<sub>3</sub>O<sub>4</sub> NS conjugation



**Figure 2.** Tumor formation in mice after the inoculation of 4T1 cells

### Statistical analysis

The obtained data were analyzed in GraphPad version 6.01, (Prism, USA) and Statistical Package for the Social Sciences (SPSS). P values less than 0.05 were regarded as statistically significant. All the analyses were performed by Two-way Analysis of Variance (ANOVA) and Tukey's post hoc test representing Mean $\pm$ SD of 5 independent experiments.

## Results

### Properties of ARE-loaded FA-CS-Fe<sub>3</sub>O<sub>4</sub> NPs

The FTIR spectrum of CS **Figure 3 A** shows the bands at 1031 and 1083 cm<sup>-1</sup> corresponding to typical stretching vibrations of C-O. The peaks of 1598 and 3445 cm<sup>-1</sup> belonged to CS were attributed to NH<sub>2</sub> and OH group, respectively. The spectrum of FA is indicated in **Figure 3 B**. The spectrum that occurred at 1638 and 1696 cm<sup>-1</sup> are the characteristics of C-O stretching vibration band in CONH and COOH groups, respectively.

In the spectra of ARE in **Figure 3 C**, the peaks of 1031, 954, and 900 cm<sup>-1</sup> correspond respectively to C-O-O-C stretching vibration in ARE. The peak of 582cm<sup>-1</sup> in blank FA-CS-Fe<sub>3</sub>O<sub>4</sub> and ARE-loaded FA-CS-Fe<sub>3</sub>O<sub>4</sub> represents for Fe<sub>3</sub>O<sub>4</sub>, and the peak of 1606cm<sup>-1</sup> is charac-

teristic of an amine group (-NH<sub>2</sub>) in CS existed in NS (**Figure 3 D and E**). In addition, the peaks of 1646 and 1699cm<sup>-1</sup> in blank FA-CS-Fe<sub>3</sub>O<sub>4</sub> and ARE-loaded FA-CS-Fe<sub>3</sub>O<sub>4</sub> are respectively indicative of C-O stretching vibration band in CONH and COOH (**Figure 3 D and E**). Moreover, the peak of 1077cm<sup>-1</sup> in ARE-loaded FA-CS-Fe<sub>3</sub>O<sub>4</sub> represents ARE (**Figure 3 E**).

The DLS analysis showed the size of 198nm and the zeta charge of -7mV for ARE loaded FA-CS-Fe<sub>3</sub>O<sub>4</sub> (**Figure 4 A**). **Figure 4 B** shows the SEM image of ARE-loaded FA-CS-Fe<sub>3</sub>O<sub>4</sub> displaying solid, dense spherical structure with an almost spherical shape.

### Drug loading consideration

Mainly, two types of drug loading are important: loading efficiency and loading capacity. Referring to the standard curve provided with different concentrations of ARE, the amount of drug entrapped in NPs could be calculated. Around 400 $\mu$ g out of 1000 $\mu$ g of ARE drug was entrapped in FA-CS-Fe<sub>3</sub>O<sub>4</sub> NPs, and 200 $\mu$ g of ARE was in 1000 $\mu$ g of total NS. In other words, the loading efficiency and the loading capacity percentages were determined as (40%) and (20%), respectively.

### Drug release pattern

The amount of free drug released from the NS at the time intervals of 2, 4, 6, 12, 24, and 48h was assessed using UV spectrophotometer. The pattern of drug release is clarified in **Figure 5**. After 48h, (97%) of drug released from NS in citrate buffer with pH of 5.4 (showing acidic pH in tumor cells) and (25%) of drug released from NS in phosphate buffer with pH of 7.4 (showing neutral pH in the blood).

### Cytotoxicity assay

The 4T1 cell lines were treated with the predetermined concentrations of 30-150 $\mu$ g/mL of ARE solution; the concentration of 150 $\mu$ g/mL of drug destroyed nearly (50%) of cells after 24h. According to the loading capacity of NPs, the concentrations were chosen in such a way that in each concentration, the NS contained (20%) ARE. As a result, the concentrations of 150-750 $\mu$ g/mL were selected. By subtracting the amount of ARE from ARE-loaded FA-CS-Fe<sub>3</sub>O<sub>4</sub>, the weight of blank FA-CS-Fe<sub>3</sub>O<sub>4</sub> NPs would be obtained (120-600 $\mu$ g/mL). Based on the concentrations of FA-CS-Fe<sub>3</sub>O<sub>4</sub> NPs used in this study, these amounts showed toxicity on 4T1 cell line due to its low-loading capacity. Although 150 $\mu$ g/mL of pure ARE killed (50%) of cells, the viability indicated that the con-

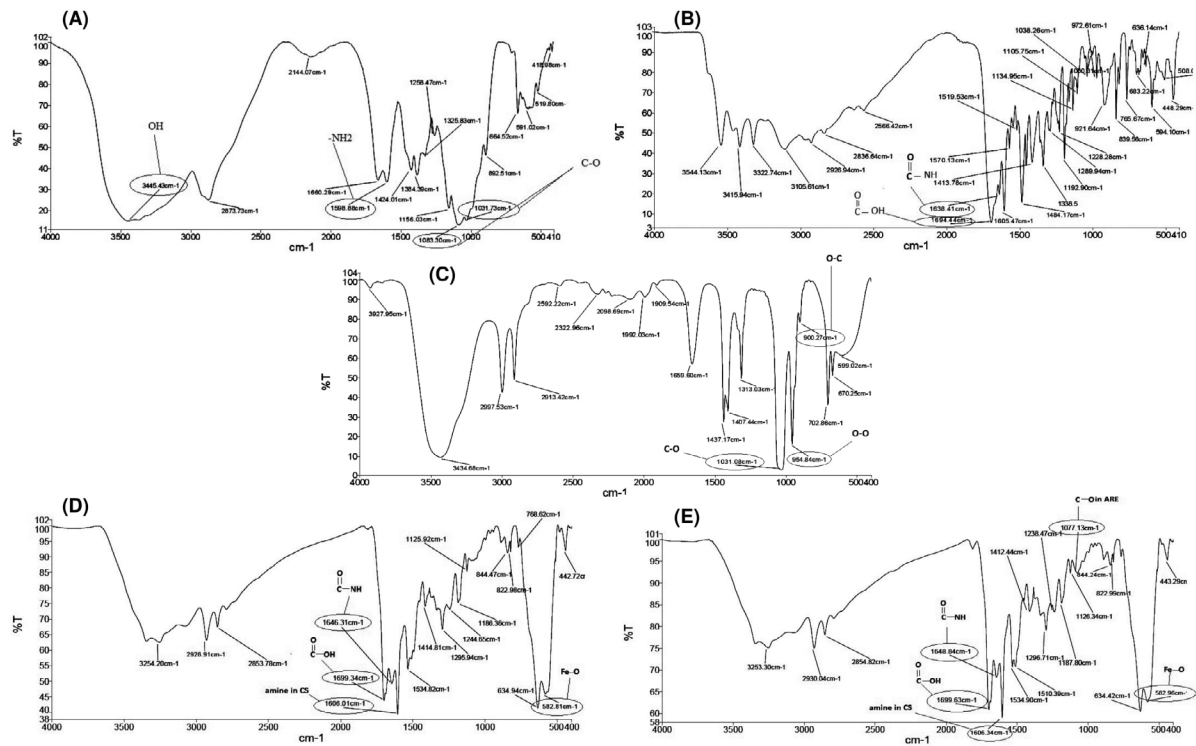


**Figure 3.** FTIR spectra of  $Fe_3O_4$ , CS, FA, ARE, FA-CS- $Fe_3O_4$  conjugate, and ARE-loaded FA-CS- $Fe_3O_4$

A: The absorption peaks of CS are shown; B: The peaks of  $1638$  and  $1694\text{cm}^{-1}$  are indicative of CO in CONH and COOH groups of FA respectively; C: The mentioned peaks represent the stretching vibration of C-O-O-C in ARE; D: The peak of  $1606$  shows amine stretching vibration in CS and the peaks of  $582\text{cm}^{-1}$  belong to Fe-O in  $Fe_3O_4$ ; E: The peak of  $1077\text{cm}^{-1}$  reveals the presence of ARE in NS

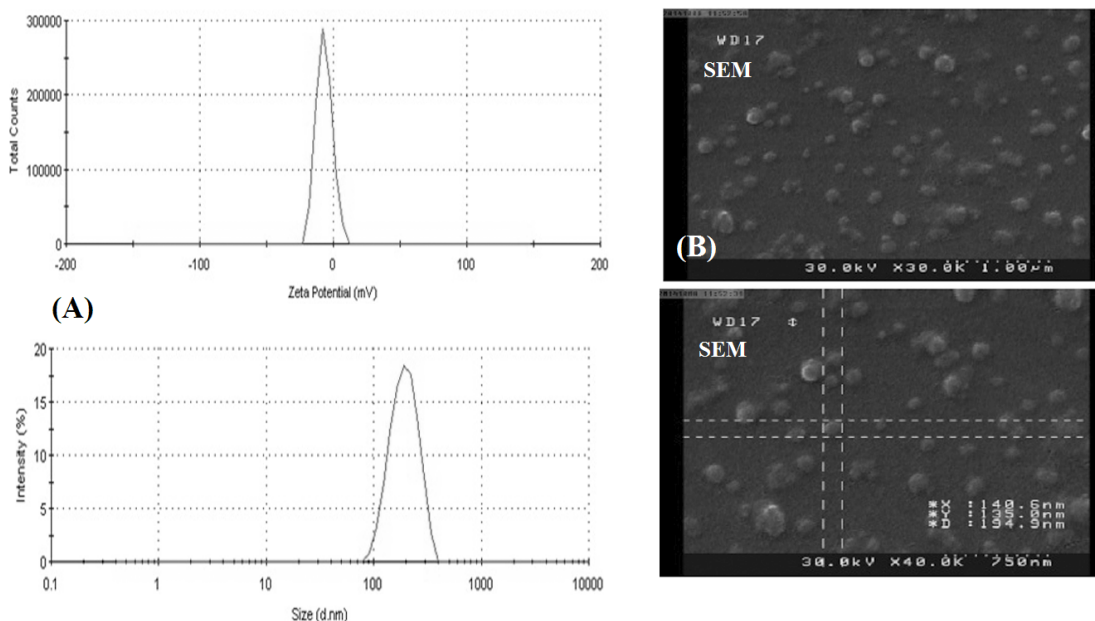
centration of NS carrying  $105\mu\text{g/mL}$  of drug would lead to the death of approximately (40%) after 24h which was totally significant compared with the drug itself and the blank NPs ( $P < 0.05$ , 2-way ANOVA). After 48h,  $75\mu\text{g/mL}$  of drug killed a little more than (50%), whereas the concentration of NS carrying  $45\mu\text{g/mL}$  of ARE solution had the same impact (Figure 6).

**Tumor volume measurement**

As shown in (Figure 7 A), the groups receiving ARE, FA-CS- $Fe_3O_4$ , and ARE-loaded FA-CS- $Fe_3O_4$  inhibited tumor growth as compared to the untreated group. Although the tumor size of the group that received NS shrank to  $94\text{mm}^3$  from the primary size of  $286\text{mm}^3$  and the experimental observations showed a decrease in tumor growth in ARE and blank FA-CS- $Fe_3O_4$  NPs treated groups as well, no significant difference was observed between the treated groups ( $P > 0.05$ , Tukey’s test).

**Cytokine assay**

As illustrated in Figure 7 B, ARE-loaded FA-CS- $Fe_3O_4$  had a remarkable impact on the generation of IFN- $\gamma$  ( $P > 0.05$ , Tukey’s test) compared with the groups receiving blank FA-CS- $Fe_3O_4$  NPs, ARE, cyclophosphamide, and PBS. It also enhanced the production of IL-4 as compared to blank FA-CS- $Fe_3O_4$  NPs, ARE, and untreated groups, whereas its production was not significant in the group received cyclophosphamide ( $P > 0.05$ , Tukey’s test). The P value for IFN- $\gamma$  in non-significant data between FA-CS- $Fe_3O_4$  and ARE was 0.242, between FA-CS- $Fe_3O_4$  and cyclophosphamide 0.828, between FA-CS- $Fe_3O_4$  and untreated 0.259, and between ARE and untreated 1. Also, the P value for IL-4 in non-significant data between ARE-loaded FA-CS- $Fe_3O_4$  and cyclophosphamide was 0.981, between FA-CS- $Fe_3O_4$  and ARE 0.798, between FA-CS- $Fe_3O_4$  and untreated group 0.705, and between ARE and untreated group 1.



IMMUNOREGULATION

**Figure 4.** The DLS analysis

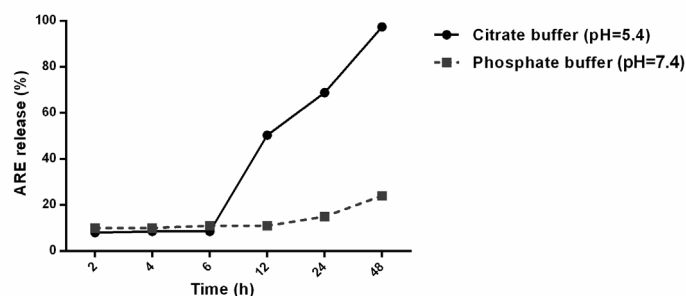
A: The size and zeta potential of ARE-loaded FA-CS-Fe<sub>3</sub>O<sub>4</sub> NS. The NS showed the average size of 198nm and the average charge of -7 mV; B: SEM of ARE loaded FA-CS-Fe<sub>3</sub>O<sub>4</sub> NS. This Figure shows the almost spherical shape of NS, and the level of disaggregation is typically shown in the picture

## Discussion

We hypothesized that the designed nanoformulation of FA-CS-Fe<sub>3</sub>O<sub>4</sub> for carrying ARE as an anti-neoplastic drug would generate a more potent response against breast cancer. Followed by our previous study on immunomodulatory effects of ARE in our department, this investigation aimed to stimulate an immune response against breast tumor by loading ARE in the designed FA-CS-Fe<sub>3</sub>O<sub>4</sub> NPs [35]. Our results imply that intraperitoneal injection of ARE loaded FA-CS-Fe<sub>3</sub>O<sub>4</sub> NPs contributes to significant type-I (Th1) immune response and anti-tumor activity in BALB/c mice with breast cancer.

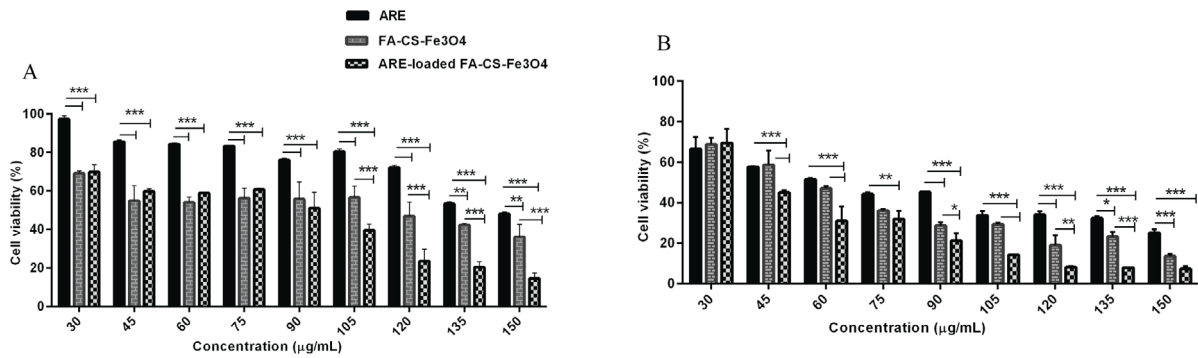
## ARE-loaded FA-CS-Fe<sub>3</sub>O<sub>4</sub> NPs

Regarding the Fe<sup>2+</sup> dependent function, similar to ARM and dihydroartemisinin as model hydrophobic chemotherapy drugs, ARE can be considered a therapeutic alternative in highly aggressive cancers by inducing mechanisms such as apoptosis and angiogenesis [36]. Accordingly, it could draw a lot of attention, if it wasn't for its hydrophobic structure, that makes it unavailable for tumor tissue. Therefore, to overcome the problem, to enhance its blood circulation time, and to concentrate it around the tumor environment, we loaded ARE in a nanoformulation with the structure of FA-CS-Fe<sub>3</sub>O<sub>4</sub>. In this structure, Fe<sub>3</sub>O<sub>4</sub> possesses sufficient capacity due



IMMUNOREGULATION

**Figure 5.** The release profile of the drug in citrate and phosphate buffer. It was observed that after passing the time of 48h, (97%) and (25%) of drug released in citrate buffer (pH 5.4) and phosphate buffer (pH 7.4), respectively



IMMUNOREGULATION

**Figure 6.** MTT cytotoxicity assay on 4T1 cell line

A: 24 h after treatment. While 150µg of pure ARE killed (50%) of cells, the viability indicates that the concentration of NS carrying 105µg of the drug caused the death of approximately (40%) after 24h which is significant in comparison with the drug itself and the blank NPs; B: 48h after treatment. 75µg of drug killed a little more than (50%), whereas the concentration of NS carrying 45µg of ARE had the same impact After 48h

to its large surface-area-to-volume ratio, which makes it more available to CS [37, 38]. Fe<sub>3</sub>O<sub>4</sub> NPs intend to aggregate because of their super paramagnetic property [39]. To reach a proper size, aggregation occurrence

would be a problematic agent. Therefore, Fe<sub>3</sub>O<sub>4</sub> was synthesized in gel-like CS solution. In this study, Fe<sub>3</sub>O<sub>4</sub> was supposed to be a cross-linker between CS polymers. CS as a biodegradable polymer is pH sensitive and can

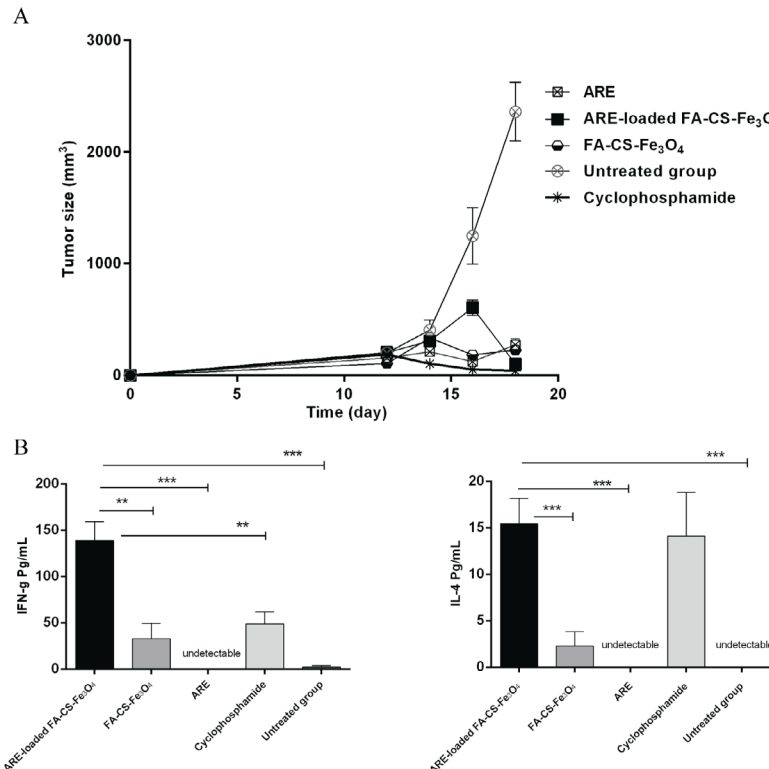


**Figure 7.** Tumor volume measurement

IMMUNOREGULATION

A: The tumor size in ARE, ARE-loaded FA-CS-Fe<sub>3</sub>O<sub>4</sub> NS, and FA-CS-Fe<sub>3</sub>O<sub>4</sub> NPs in comparison with cyclophosphamide and the untreated group. The difference in the volume of tumor between the treated groups was not significant. The treated groups shrank the tumor size in comparison with the untreated group, and according to the graph, the difference in the reduction of tumor growth was significant; B: The assay of IFN-γ and IL-4 cytokines by ELISA. ARE-loaded FA-CS-Fe<sub>3</sub>O<sub>4</sub> NS increased the level of IFN-γ significantly as compared to the other groups. The NS enhanced the level of IL-4 cytokine as well, but IFN-γ increase in proportion to IL-4 enhancement was a lot more significant in the group received NS

be degraded in acidic pH of tumor environment and endolysosomes of tumor cells [40]. Thus, it could be an excellent candidate to release the drug in acidic pH around or within the tumor cells. To demonstrate the formation and the presence of  $\text{Fe}_3\text{O}_4$  in NS (Figure 3), the IR spectrum of  $582\text{cm}^{-1}$  was obvious evidence compared with other studies [28, 41]. Moreover, the peak of  $1534\text{cm}^{-1}$ , which is near to the spectrum mentioned in another study is characteristic of the amine group in CS [42]. To direct the obtained NPs to the tumor tissue, another component like FA was applied. Tumor cells have a great deal of FA receptors on the surface compared with normal cells [43, 44]. Hence, by receptor-mediated endocytosis, the NS would be able to pass through the tumor cells and make ARE more available to the tumor site. As mentioned, the peaks of  $1638$  and  $1694\text{cm}^{-1}$  are characteristics of ketone group binding NH and ketone binding OH, respectively. Accordingly, the peaks of  $1646$  and  $1699$  represent the existence of FA in the NS [45].

In this study, the average size of  $198\text{nm}$  with the charge of  $-7\text{mV}$  were achieved (Figure 4 A). Primarily, particles less than  $300\text{nm}$  (less than  $750\text{nm}$  in some studies) enter through the leaky endothelial cells of tumor vessels, and such regular array of endothelial cells do not exist in tumor tissue; this is a common event which occurs with increasing angiogenesis [46]. By nanoemulsifying of ARE in one study, the size of  $156\text{nm}$  was achieved, while the potential charge was more negative  $-23\text{mV}$  [47]. The more positive charge the particles have, the more contact attachment between particles and tumor cells might happen [48]. The micrographs obtained by SEM did not show any aggregated particles, and also they had a compact spherical shape (Figure 4 B). The biocompatibility and cellular uptake are probably influenced by the shape of nanomaterials. Dendrimer-shaped or plate-shaped particles showed more toxicity than spherical-shaped NPs on normal cells [49]. All the mentioned studies showed that we achieved a proper size, with zeta potential, and suitable shape.

### Loading and release profile of ARE

The loading capacity exhibited that the NS can load only (20%) of its total mass and also (40%) of the total drug used. It is to say that every  $1000\mu\text{g}$  of total NS contained  $200\mu\text{g}$  ARE and by consuming  $1000\mu\text{g}$  ARE,  $400\mu\text{g}$  would be entrapped in FA-CS- $\text{Fe}_3\text{O}_4$  NPs. In another study performed on carrying doxorubicin by FA-CS- $\text{Fe}_3\text{O}_4$  NPs, drug loading of about (10%) was reported [50]. These blank NPs were able to physically entrap low amounts of ARE (20%) in our study too. Therefore, for reaching the effective dose for tumor growth reduction,

high quantities of NS were applied in vitro, which might be toxic. In another study, to carry ARE and increase its blood circulation time for malaria treatment, solid lipid NPs were used [51]. The entrapment efficiency was recorded precisely like the amount obtained in our study "loading efficiency of (40%)", but no reporting on its release profile was reported in the mentioned study.

To evaluate the release profile of ARE from the NPs for 48h (Figure 5), at the determined time intervals, one set was quantified spectrophotometrically. According to the release profile in our study, a rapid release of ARE from FA-CS- $\text{Fe}_3\text{O}_4$  appeared at pH 5.4, and (97%) of ARE was released into citrate buffer with pH 5.4, while a prolonged release of drug was observed in phosphate buffer with pH 7.4 after 48h. This amount of release is indicative of the designed NS excellent pH sensitivity. This pH-dependent release of ARE is of great value in clinical use because the extracellular microenvironment and intracellular lysosomes of tumor cells are both acidic [52].

### Assessment of cytotoxicity in tumor cells

By using different concentrations ( $30$ - $150\mu\text{g}/\text{mL}$ ) of ARE (Figure 6), the dose which killed about (50%) of 4T1 cells was achieved ( $150\mu\text{g}/\text{mL}$ ). To contain (20%) ARE, the concentration range of  $150$ - $750\mu\text{g}/\text{mL}$  of NS was chosen. Because of the high amount, free-drug NPs showed toxicity on 4T1 cells. In another study, it was shown that  $\text{Fe}_3\text{O}_4$  NPs at higher concentrations (more than  $300\mu\text{g}/\text{mL}$ ) would lead to toxicity for up to 6 hours of exposure [53]. Although the same amount of  $\text{Fe}_3\text{O}_4$  NPs was not used in this study, the prolonged exposure (24h and 48h) of free-drug NPs ( $120$ - $600\mu\text{g}/\text{mL}$ ) reduced the viability to about (70-40%). Accordingly, the NS showed more toxicity on 4T1 cells, and in the concentration containing  $105\mu\text{g}/\text{mL}$  of ARE, the NS reduced the viability to (40%).

### Tumor volume measurement

The adequate concentration of ARE-loaded NPs with the lowest probable toxic effects should be selected for injection to mice bearing breast cancer. Referring to one study performed in 2012 by Ping Ma et al., 5 and  $10\text{mg}/\text{kg}$  of pure  $\text{Fe}_3\text{O}_4$  was recommended as the safest dose with the lowest side effects [54]. As  $20\text{mg}/\text{kg}$  of the NS in this investigation contained the components of ARE, CS, and FA along with  $\text{Fe}_3\text{O}_4$ , it seems that the choice of this amount was a reasonable selection. Of course,  $20\text{mg}/\text{kg}$  of NS possessed undoubtedly less ARE in comparison with solo ARE in the same dose. This condition elucidates

that ARE loaded FA-CS-Fe<sub>3</sub>O<sub>4</sub> NPs owning less drug had the same output on tumor growth (Figure 7). Despite no notable difference between ARE and ARE-loaded NP in the growth of the tumor on day 18, the latter specified similar impact as compared to cyclophosphamide on the growth of cancer. Along with our investigation, another similar study applied liposome nanomagnetic for carrying ARM and targeted this NS to the breast tumor tissue in BALB/c mice [55]. However, carrying ARE, ether derivative, and modified form of ARM, with nanoformulation of FA-CS-Fe<sub>3</sub>O<sub>4</sub> to target tumor cells, was performed for the first time in this study.

### Assessment of cytokine production

Following NS injection, a significant enhancement in the secretion level of IFN- $\gamma$  was observed (Figure 7 B). In our previous study, it had been suggested that ARE by its own is not able enough to trigger an immune response from the insight of IFN- $\gamma$  and IL-4 cytokines' secretion [35]. Although solo ARE also showed no effects on the generation of these two cytokines in our research, notable results in immune response after NS injection were reported compared with the control group. It is supposed that there was a possible link between raised IFN- $\gamma$  and dropped tumor growth [56]. Th1 orientation in the microenvironment of the tumor provides an appropriate condition for anti-tumor responses. Although ARE-loaded FA-CS-Fe<sub>3</sub>O<sub>4</sub> NPs increased the rate of both IFN- $\gamma$  and IL-4, IFN- $\gamma$  enhancement in proportion to IL-4 was a lot more significant in the group receiving NS. That is another evidence for the effectiveness of NS as a therapeutic drug on the induction of Th1 immune response besides its tumor-killing characteristics. Considering the results obtained in the present study, ARE-loaded FA-CS-Fe<sub>3</sub>O<sub>4</sub> NPs can have a promising therapeutic effect on the reduction of tumor growth and increase in the stimulation of immune responders more likely to Th1.

As it is shown in our study and previous studies, ARE showed cytotoxic effects on tumor cells. Therefore, it can be regarded as an anti-cancer drug. But the problem is its low availability in the tumor site. In this study, we tried to concentrate it in tumor site and inside of a tumor cell through our designed NS. So, it would be promising to kill more tumor cells. After killing tumor cell and lysing, more antigens and peptides are released around the tumor site. In this area, there are some immune cells like dendritic cells which are capable of taking these antigens and presenting it to T cells in tumor site or lymphoid organs. As a result, more T cells would be activated, and the concentration of IFN- $\gamma$  be enhanced eventually.

Our findings showed that ARE-loaded FA-CS-Fe<sub>3</sub>O<sub>4</sub> NP with the designed formulation decreased the rate of tumor growth and increased the level of IFN- $\gamma$  in mice with breast cancer. The inhibitory mechanisms of tumor growth should be studied further. More analysis on the effect of these NPs on normal cells, cytokine patterns, tumor infiltrated lymphocytes, a variety of immune cells, and intracellular signaling system in murine models should be performed. Regarding all findings in this study, ARE-loaded FA-CS-Fe<sub>3</sub>O<sub>4</sub> NP can be considered as a promising nano-drug delivery system for the treatment of breast cancer.

### Ethical Considerations

#### Compliance with ethical guidelines

All experiments were performed on mice in compliance with the guidelines of the Medical Ethics Committee of Tarbiat Modares University (No. D52-6854).

#### Funding

This study was supported by funds from Tarbiat Modares University

#### Authors' contributions

Conceptualization, methodology, supervision: Hajar Rajaei, Zuhair Mohammad Hassan; Investigation, writing-original draft: Hajar Rajaei; Writing-review and editing: Hajar Rajaei, Mirza Ali Mofazzal Jahromi, Nima Khoramabadi, Zuhair Mohammad Hassan; Funding acquisition: Zuhair Mohammad Hassan.

#### Conflicts of interest

Authors declared no conflicts of interest.

#### Acknowledgements

The authors express their gratitude to the Tarbiat Modares University for facilitating implementation and securing the fund.

### References

- [1] Kumar S, Singh RK, Sharma R, Murthy R, Bhardwaj T. Design, synthesis and evaluation of antimalarial potential of polyphosphazene linked combination therapy of primaquine and dihydroartemisinin. *European Journal of*

- Pharmaceutical Sciences. 2015; 66:123-37. [DOI:10.1016/j.ejps.2014.09.023] [PMID]
- [2] Omoyeni OA, Hussein AA, Iwuoha E, Green IR. A review of the ethnomedicinal uses, phytochemistry and pharmacology of the *Pleiocarpa* genus. *Phytochemistry Reviews*. 2017; 16(1):97-115.
- [3] Efferth T, Olbrich A, Bauer R. mRNA expression profiles for the response of human tumor cell lines to the antimalarial drugs artesunate, arteether, and artemether. *Biochemical Pharmacology*. 2002; 64(4):617-23. [DOI:10.1016/S0006-2952(02)01221-2]
- [4] Miller LH, Su X. Artemisinin: Discovery from the Chinese herbal garden. *Cell*. 2011; 146(6):855-8. [DOI:10.1016/j.cell.2011.08.024] [PMID] [PMCID]
- [5] Michaelsen F-W, Saeed ME, Schwarzkopf J, Efferth T. Activity of *Artemisia annua* and artemisinin derivatives, in prostate carcinoma. *Phytomedicine*. 2015; 22(14):1223-31. [DOI:10.1016/j.phymed.2015.11.001] [PMID]
- [6] Lu JJ, Meng LH, Shankavaram UT, Zhu CH, Tong LJ, Chen G, et al. Dihydroartemisinin accelerates c-MYC oncoprotein degradation and induces apoptosis in c-MYC-overexpressing tumor cells. *Biochemical Pharmacology*. 2010; 80(1):22-30. [DOI:10.1016/j.bcp.2010.02.016] [PMID]
- [7] Morrissey C, Gallis B, Solazzi JW, Kim BJ, Gulati R, Vakar-Lopez F, et al. Effect of artemisinin derivatives on apoptosis and cell cycle in prostate cancer cells. *Anticancer Drugs*. 2010; 21(4):423-32. [DOI:10.1097/CAD.0b013e328336f57b] [PMID] [PMCID]
- [8] Lai H, Sasaki T, Singh NP, Messay A. Effects of artemisinin-tagged holotransferrin on cancer cells. *Life Sciences*. 2005; 76(11):1267-79. [DOI:10.1016/j.lfs.2004.08.020] [PMID]
- [9] Efferth T. Molecular pharmacology and pharmacogenomics of artemisinin and its derivatives in cancer cells. *Current Drug Targets*. 2006;7(4):407-21. [DOI:10.2174/138945006776359412] [PMID]
- [10] Singh NP, Lai HC. Artemisinin induces apoptosis in human cancer cells. *Anticancer Research*. 2004; 24(4):2277-80. [PMID]
- [11] Tran TH, Nguyen AN, Kim JO, Yong CS, Nguyen CN. Enhancing activity of artesunate against breast cancer cells via induced-apoptosis pathway by loading into lipid carriers. *Artificial Cells, Nanomedicine, and Biotechnology*. 2016; 44(8):1979-87. [DOI:10.3109/21691401.2015.1129616] [PMID]
- [12] Xu C-C, Deng T, Fan M-L, Lv W-B, Liu J-H, Yu B-Y. Synthesis and in vitro antitumor evaluation of dihydroartemisinin-cinnamic acid ester derivatives. *European Journal of Medicinal Chemistry*. 2016; 107:192-203. [DOI:10.1016/j.ejmech.2015.11.003] [PMID]
- [13] Kjaer A, Verstappen F, Bouwmeester H, Ivarsen E, Frette X, Christensen LP, et al. Artemisinin production and precursor ratio in full grown *Artemisia annua* L. plants subjected to external stress. *Planta*. 2013; 237(4):955-66. [DOI:10.1007/s00425-012-1811-y] [PMID]
- [14] Ferreira JF, Luthria DL, Sasaki T, Heyerick A. Flavonoids from *Artemisia annua* L. as antioxidants and their potential synergism with artemisinin against malaria and cancer. *Molecules*. 2010; 15(5):3135-70. [DOI:10.3390/molecules15053135] [PMID] [PMCID]
- [15] Ghantous A, Gali-Muhtasib H, Vuorela H, Saliba NA, Darwiche N. What made sesquiterpene lactones reach cancer clinical trials? *Drug Discovery Today*. 2010; 15(15-16):668-78. [DOI:10.1016/j.drudis.2010.06.002] [PMID]
- [16] Bystrom LM, Guzman ML, Rivella S. Iron and reactive oxygen species: Friends or foes of cancer cells? *Antioxidants & Redox Signaling*. 2014; 20(12):1917-24. [DOI:10.1089/ars.2012.5014] [PMID] [PMCID]
- [17] Gatter KC, Brown G, Trowbridge I, Woolston R, Mason D. Transferrin receptors in human tissues: Their distribution and possible clinical relevance. *Journal of Clinical Pathology*. 1983; 36(5):539-45. [DOI:10.1136/jcp.36.5.539] [PMID] [PMCID]
- [18] Esserman L, Takahashi S, Rojas V, Warnke R, Levy R. An epitope of the transferrin receptor is exposed on the cell surface of high-grade but not low-grade human lymphomas. *Blood*. 1989; 74(8):2718-29. [PMID]
- [19] Grivennikov SI, Greten FR, Karin M. Immunity, inflammation, and cancer. *Cell*. 2010; 140(6):883-99. [DOI:10.1016/j.cell.2010.01.025] [PMID] [PMCID]
- [20] Wang B, Zaidi N, He L-Z, Zhang L, Kuroiwa JM, Keler T, et al. Targeting of the non-mutated tumor antigen HER2/neu to mature dendritic cells induces an integrated immune response that protects against breast cancer in mice. *Breast Cancer Research*. 2012; 14(2):R39. [DOI:10.1186/bcr3135] [PMID] [PMCID]
- [21] Gupta S, Chadha R. Studies on the preparation and evaluation of antimalarial activity of arteether and complexed arteether with  $\beta$ -CD loaded chitosan/lecithin nanoparticles. *Pharmaceutical Nanotechnology*. 2013;1(3):204-12. [DOI:10.2174/22117385113019990004]
- [22] Dhankhar R, Vyas SP, Jain AK, Arora S, Rath G, Goyal AK. Advances in novel drug delivery strategies for breast cancer therapy. *Artificial Cells, Blood Substitutes, And Immobilization Biotechnology*. 2010; 38(5):230-49. [DOI:10.3109/10731199.2010.494578] [PMID]
- [23] Polyak B, Friedman G. Magnetic targeting for site-specific drug delivery: Applications and clinical potential. *Expert Opinion on Drug Delivery*. 2009; 6(1):53-70. [DOI:10.1517/17425240802662795] [PMID]
- [24] Arruebo M, Fernández-Pacheco R, Ibarra MR, Santamaría J. Magnetic nanoparticles for drug delivery. *Nano Today*. 2007; 2(3):22-32. [DOI:10.1016/S1748-0132(07)70084-1]
- [25] Mody VV, Cox A, Shah S, Singh A, Bevins W, Parihar H. Magnetic nanoparticle drug delivery systems for targeting tumor. *Applied Nanoscience*. 2014; 4(4):385-92. [DOI:10.1007/s13204-013-0216-y]
- [26] Wang Y, Han Y, Yang Y, Yang J, Guo X, Zhang J, et al. Effect of interaction of magnetic nanoparticles of  $\text{Fe}_3\text{O}_4$  and artesunate on apoptosis of K562 cells. *International Journal of Nanomedicine*. 2011; 6:1185-92. [DOI:10.2147/IJN.S19723] [PMID] [PMCID]
- [27] Ankanwar B, Lai T, Huang J, Liu R, Hsiao M, Chen C, et al. Biocompatibility of  $\text{Fe}_3\text{O}_4$  nanoparticles evaluated by in vitro cytotoxicity assays using normal, glia and breast cancer cells. *Nanotechnology*. 2010; 21(7):75102. [DOI:10.1088/0957-4484/21/7/075102] [PMID]

- [28] Qu J-B, Shao H-H, Jing G-L, Huang F. PEG-chitosan-coated iron oxide nanoparticles with high saturated magnetization as carriers of 10-hydroxycamptothecin: Preparation, characterization and cytotoxicity studies. *Colloids and Surfaces B: Biointerfaces*. 2013; 102:37-44. [DOI:10.1016/j.colsurfb.2012.08.004] [PMID]
- [29] Qi LF, Xu ZR, Li Y, Jiang X, Han XY. In vitro effects of chitosan nanoparticles on proliferation of human gastric carcinoma cell line MGC803 cells. *World Journal of Gastroenterology*. 2005; 11(33):5136-41. [DOI:10.3748/wjg.v11.i33.5136] [PMID] [PMCID]
- [30] Zhang H, Mardiyani S, Chan WC, Kumacheva E. Design of biocompatible chitosan microgels for targeted pH-mediated intracellular release of cancer therapeutics. *Biomacromolecules*. 2006; 7(5):1568-72. [DOI:10.1021/bm050912z] [PMID]
- [31] Hilgenbrink AR, Low PS. Folate receptor-mediated drug targeting: From therapeutics to diagnostics. *Journal of Pharmaceutical Sciences*. 2005; 94(10):2135-46. [DOI:10.1002/jps.20457] [PMID]
- [32] Kamen BA, Smith AK. A review of folate receptor alpha cycling and 5-methyltetrahydrofolate accumulation with an emphasis on cell models in vitro *Advanced Drug Delivery Reviews*. 2004; 56(8):1085-97. [DOI:10.1016/j.addr.2004.01.002] [PMID]
- [33] Bisht S, Feldmann G, Soni S, Ravi R, Karikar C, Maitra A, et al. Polymeric nanoparticle-encapsulated curcumin ("nanocurcumin"): A novel strategy for human cancer therapy. *Journal of Nanobiotechnology*. 2007; 5:3. [DOI:10.1186/1477-3155-5-3] [PMID] [PMCID]
- [34] Zhuang Q, Hong F, Shen A, Zheng L, Zeng J, Lin W, et al. Pien Tze Huang inhibits tumor cell proliferation and promotes apoptosis via suppressing the STAT3 pathway in a colorectal cancer mouse model. *International Journal of Oncology*. 2012; 40(5):1569-74. [DOI:10.3892/ijo.2012.1326] [PMID]
- [35] Azimi Mohammadabadi M, Hassan ZM, Hosseini AZ, Noori S, Mahdavi M, Maroofzadeh S, et al. Study of immunomodulatory effects of arteether administrated intratumorally. *Iranian Journal of Allergy, Asthma and Immunology*. 2013; 12(1):57-62. [DOI: 012.01/ijaa.5762] [PMID]
- [36] Singh NP, Lai H. Selective toxicity of dihydroartemisinin and holotransferrin toward human breast cancer cells. *Life Sciences*. 2001; 70(1):49-56. [DOI:10.1016/S0024-3205(01)01372-8]
- [37] Chen FH, Zhang LM, Chen QT, Zhang Y, Zhang ZJ. Synthesis of a novel magnetic drug delivery system composed of doxorubicin-conjugated Fe<sub>3</sub>O<sub>4</sub> nanoparticle cores and a PEG-functionalized porous silica shell. *Chemical Communications (Cambridge)*. 2010; 46(45):8633-5. [DOI:10.1039/c0cc02577a] [PMID]
- [38] Gupta AK, Gupta M. Synthesis and surface engineering of iron oxide nanoparticles for biomedical applications. *Biomaterials*. 2005; 26(18):3995-4021. [DOI:10.1016/j.biomaterials.2004.10.012] [PMID]
- [39] Gun S, Edirisinghe M, Stride E. Encapsulation of superparamagnetic iron oxide nanoparticles in poly-(lactide-co-glycolic acid) microspheres for biomedical applications. *Materials Science & Engineering, C, Materials for Biological Applications*. 2013; 33(6):3129-37. [DOI:10.1016/j.msec.2013.03.001] [PMID]
- [40] Deng Z, Zhen Z, Hu X, Wu S, Xu Z, Chu PK. Hollow chitosan-silica nanospheres as pH-sensitive targeted delivery carriers in breast cancer therapy. *Biomaterials*. 2011; 32(21):4976-86. [DOI:10.1016/j.biomaterials.2011.03.050] [PMID]
- [41] Li Z, Wei L, Gao M, Lei H. One-pot reaction to synthesize biocompatible magnetite nanoparticles. *Advanced Materials*. 2005; 17(8):1001-5. [DOI:10.1002/adma.200401545]
- [42] Hu X-j, Liu Y, Zhou X-f, Zhu Q-l, Bei Y-y, You B-g, et al. Synthesis and characterization of low-toxicity N-caprinoyl-N-trimethyl chitosan as self-assembled micelles carriers for osteole. *International Journal of Nanomedicine*. 2013; 8:3543-58. [DOI:10.2147/IJN.S46369] [PMID] [PMCID]
- [43] Low PS, Henne WA, Doorneweerd DD. Discovery and development of folic-acid-based receptor targeting for imaging and therapy of cancer and inflammatory diseases. *Accounts of Chemical Research*. 2008; 41(1):120-9. [DOI:10.1021/ar7000815] [PMID]
- [44] Brannon-Peppas L, Blanchette JO. Nanoparticle and targeted systems for cancer therapy. *Advanced Drug Delivery Reviews*. 2004; 56(11):1649-59. [DOI:10.1016/j.addr.2004.02.014] [PMID]
- [45] Sahu SK, Mallick SK, Santra S, Maiti TK, Ghosh SK, Pramanik P. In vitro evaluation of folic acid modified carboxymethyl chitosan nanoparticles loaded with doxorubicin for targeted delivery. *Journal of Materials Science. Materials in Medicine*. 2010; 21(5):1587-97. [DOI:10.1007/s10856-010-3998-4] [PMID]
- [46] Campbell RB. Tumor physiology and delivery of nanopharmaceuticals. *Anti-cancer Agents in Medicinal Chemistry*. 2006; 6(6):503-12. [DOI:10.2174/187152006778699077] [PMID]
- [47] Dwivedi P, Khatik R, Chaturvedi P, Khandelwal K, Taneja I, Raju KSR, Dwivedi H, kumar Singh S, Gupta PK, Shukla P. Arteether nanoemulsion for enhanced efficacy against *Plasmodium yoelii nigeriensis* malaria: An approach by enhanced bioavailability. *Colloids and Surfaces B: Biointerfaces*. 2015; 126:467-75. [DOI:10.1016/j.colsurfb.2014.12.052] [PMID]
- [48] Grossman JH, McNeil SE. Nanotechnology in cancer medicine. *Physics Today*. 2012; 65(8):1-38. [DOI:10.1063/PT.3.1678]
- [49] Lin PC, Lin S, Wang PC, Sridhar R. Techniques for physicochemical characterization of nanomaterials. *Biotechnology Advances*. 2014; 32(4):711-26. [DOI:10.1016/j.biotechadv.2013.11.006] [PMID] [PMCID]
- [50] Zarrin A, Sadighian S, Rostamizadeh K, Firuzi O, Hamidi M, Mohammadi-Samani S, et al. Design, preparation, and in vitro characterization of a trimodally-targeted nanomagnetic onco-theranostic system for cancer diagnosis and therapy. *International Journal of Pharmaceutics*. 2015; 500(1-2):62-76. [DOI:10.1016/j.ijpharm.2015.12.051] [PMID]
- [51] Dwivedi P, Khatik R, Khandelwal K, Shukla R, Paliwal SK, Dwivedi AK, et al. Preparation and characterization of solid lipid nanoparticles of antimalarial drug arteether for oral administration. *Journal of Biomaterials and Tissue Engineering*. 2014; 4(2):133-7. [DOI:10.1166/jbt.2014.1148]

- [52] Estrella V, Chen T, Lloyd M, Wojtkowiak J, Cornell HH, Ibrahim-Hashim A, et al. Acidity generated by the tumor microenvironment drives local invasion. *Cancer Research*. 2013; 73(5):1524-35. [DOI:10.1158/0008-5472.CAN-12-2796] [PMID] [PMCID]
- [53] Naqvi S, Samim M, Abdin M, Ahmed FJ, Maitra A, Prashant C, et al. Concentration-dependent toxicity of iron oxide nanoparticles mediated by increased oxidative stress. *International Journal of Nanomedicine*. 2010; 5:983-9. [DOI:10.2147/IJN.S13244] [PMID] [PMCID]
- [54] Ma P, Luo Q, Chen J, Gan Y, Du J, Ding S, et al. Intraperitoneal injection of magnetic Fe<sub>3</sub>O<sub>4</sub>-nanoparticle induces hepatic and renal tissue injury via oxidative stress in mice. *International Journal of Nanomedicine*. 2012; 7:4809-18. [DOI:10.2147/IJN.S34349] [PMID] [PMCID]
- [55] Gharib A, Faezizadeh Z, Mesbah-Namin SA, Saravani R. Experimental treatment of breast cancer-bearing BALB/c mice by artemisinin and transferrin-loaded magnetic nanoliposomes. *Pharmacognosy magazine*. 2015; 11(suppl. 1):S117-22. [DOI:10.4103/0973-1296.157710] [PMID] [PMCID]
- [56] Rosenberg SA, Yang JC, Restifo NP. Cancer immunotherapy: Moving beyond current vaccines. *Nature Medicine*. 2004; 10(9):909-15. [DOI:10.1038/nm1100] [PMID] [PMCID]

---

This Page Intentionally Left Blank

---